ac magnetic hysteresis loops of Bi-Sr-Ca-Cu-O 110-K-phase superconductors and the effect of microstructural alteration

N. Harish Kumar and V. Seshu Bai
School of Physics, University of Hyderabad, Hyderabad-500 046, India
(Received 13 November 1995)

The field variations of ac M-H loops are recorded at 77 K and 33 Hz using a lock-in flat-band detection method in sintered and press sintered 110-K-phase samples of the Bi-Sr-Ca-Cu-O system. From the slope of the M vs H_m curve the flux profiles and the effective relative permeability ($\mu_{\rm cer}$) of the samples are determined. Using this value of $\mu_{\rm cer}$ the intergrain and intragrain contributions to the magnetization are separated out. The intergranular loops of the sintered sample could be simulated very well using Kim's model, while for the press-sintered sample the exponential model gives a better fit. Our results show that the loop closure exhibited by the intergranular loop can be simulated to the critical state models without subtracting the wing portion in contrast to the Dersch-Blatter approach. The intragranular loops of sintered samples show quite a good fit to the exponential model after introducing the surface barrier modification. The intergranular critical current density (J_{ci}) and the apparent lower critical field (H_{c1g}) of the grains are found to be enhanced due to press sintering. The field variations of the various physical quantities obtained from the loops are analyzed to see the effect of microstructural alterations introduced by the press-sintering method. By doing a fast Fourier transform on the M vs t curve the harmonic components are separated out and their variation with the ac field amplitude is studied. [S0163-1829(96)04018-0]

I. INTRODUCTION

The magnetic properties and the current transport in granular superconductors are governed by not only the nature of the diamagnetic grains but also their interconnections which constitute the superconducting matrix.[1–3] The size and distribution of the interconnections and their properties will greatly depend on the processing method used. For instance melt processing of $YBa_2Cu_3O_{7-\delta}$ and introducing pinning centers is known[4] to enhance the critical current density (J_c). Similarly press sintering is reported[5] to improve the J_c in Bi-Sr-Ca-Cu-O (BSCCO) system.

ac susceptibility measurement is widely used[6–11] to characterize the ceramic high-T_c superconductors (HTS's) and to estimate the intergranular critical current densities. The magnetic response of HTS's is better described by ac magnetization studies rather than the fundamental component of ac susceptibility since the former includes the harmonic components as well. Compared to ac susceptibility measurements, reports on ac magnetic hysteresis studies are very few in the literature.

Grover *et al.*[12] recorded the field and temperature variation of M-H loops in sintered $YBa_2Cu_3O_{7-\delta}$ (YBCO) samples using an electronic integrator method and analyzed them by assuming an exponential functional dependence for J_c on field. Edmond and Firth[13] also used a similar method and analyzed their data using Kim's model. Maury *et al.*[14] studied the grain size dependence of the hysteresis loops in YBCO recorded using an analog-to-digital (A/D) converter. Navarro *et al.*[15] generated the full hysteresis loops by recording the first nine components of the harmonic susceptibilities individually and then reconstructing the full loop. Fabricatore *et al.*[16] studied the magnetization and the penetrated and trapped flux using a three-channel waveform recorder followed by numerical integration. Ghatak *et al.*[17] studied the ac magnetization and harmonic behavior of pure and silver-doped YBCO sintered samples. Gömöry[18] and Gough *et al.*[19] have reported a lock-in flat-band detection method for recording ac M-H loops and this is based on Campbell's technique[20] reported to study flux penetration in conventional superconductors. Gough *et al.*[19] have analyzed the loops by assuming functional dependences for J_c on field of the form $J_c(0)[h/(H+h)]$ and $J_c(0)\exp[-\ln 2(H/h)]$ where $J_c(0)$ is the critical current density in zero field and h is the field that would suppress the critical current to half its zero-field value.

By far the $YBa_2Cu_3O_{7-\delta}$ system is the most extensively studied[21–26] among the HTS's in bulk polycrystalline form. In the BSCCO system out of the two phases with their T_c's above the boiling point of liquid nitrogen (85 K phase and the 110 K phase), the 110 K phase has been studied to a lesser extent due to the difficulty in synthesizing it in a stable and single-phase form. Attempts to stabilize this phase by the addition of Pb or Sb have often yielded multiphase compounds.[27–29] Shi *et al.*[30] reported that this phase can be prepared in a stable and single-phase form from the starting composition $Bi_{1.6}Pb_{0.4}Sr_2Ca_2Cu_3O_y$ after intermediate cold working. A detailed study of this system by our group[31] led to the identification of the starting composition $Bi_{1.2}Pb_{0.3}Sr_{1.5}Ca_2Cu_3O_y$ (which is deficient in Bi and Sr compared to the $Bi_2Sr_2Ca_2Cu_3O_y$ reported often in the literature) to prepare this compound in a stable and single-phase form without intermediate cold working. Repeated cold uniaxial pressing and sintering sequences (press-sintering method) alter the microstructure and are reported to result in enhanced J_c. We present here a detailed investigation of the ac magnetic hysteresis measurements in sintered and press-sintered $Bi_{1.2}Pb_{0.3}Sr_{1.5}Ca_2Cu_3O_y$ (samples A and B) with the aim to

investigate the magnetic properties of the intergranular matrix as well as that of the grains.

II. SAMPLE AND MEASUREMENT DETAILS

Methods of synthesizing the sintered and press-sintered BSCCO 110-K-phase superconductors and their characterization using x-ray diffraction (XRD), temperature variation of electrical resistivity (ρ vs T), and temperature and field variation of ac susceptibility (χ vs T, χ vs H) studies are reported in Refs. 31 and 10. From the ρ vs T measurements the $T_c(0)$ values are found to be 106.4 K and 105.9 K for sample A and sample B, respectively. The susceptibility and XRD measurements show no traces of the 85 K phase in both the samples. The XRD results[31] showed texturing along the c axis of the unit cell in the press-sintered sample. The scanning electron micrographs (SEM's) of the fractured surface showed that sample A is highly porous while the porosity has reduced on press sintering. The average size of the grains which is of ~ 5 μm in sample A gets reduced to 1 μm in sample B. From a comparison of the measured densities to the theoretical values, the porosity is determined to be 50% and 15% for samples A and B, respectively. The samples used are of cylindrical geometry with lengths 14.33 and 14.25 mm and diameters 1.16 and 0.98 mm, respectively. The demagnetizing factors (D) for the samples were obtained using the table in Ref. 32 and are 0.067 for sample A and 0.055 for sample B.

Earlier study of fundamental intergranular ac susceptibility[10] showed that the temperature and field dependences of χ_1' and χ_1'' can be simulated to Kim's model in sample A and are closer to Bean's model for sample B. In this paper, the field dependence of the total magnetization that includes the contribution also from the harmonics is investigated. The applicability of critical state models is examined and the field dependence of various quantities is derived, as described below.

III. ac MAGNETIC HYSTERESIS LOOP MEASUREMENTS

To study the hysteretic magnetization of HTS's, the output of a mutual inductance coil assembly, consisting of a pair of identical secondary coils wound in opposition and placed inside a coaxial primary solenoid, is integrated and recorded as a function of field amplitude. When the sample is placed in one of the secondary coils the resultant output of secondaries is proportional to the rate of change of magnetization (dM/dt) of the sample by integrating which we get the magnetization of the sample. The integration can be done either by using an electronic integrator[12,13,17] or by recording the dM/dt signal and then numerically integrating it.[14,16] Gömöry[18] and Gough *et al.*[19] have reported a phase sensitive detector (PSD) method in which a lock-in analyzer operated in the flat-band mode is used for performing the integration. The lock-in analyzer when operated in this mode provides an accurate integration of the dM/dt signal (at any point of the phase set in the lock in) by multiplying it with a square wave derived from the reference and averaging the product over one period of the ac field. The lock-in output is proportional to

$$\int_{\phi}^{\phi+2\pi} \frac{dM}{dt}\, dt = M(\phi+\pi) - M(\phi) = -2M(\phi), \quad (1)$$

where ϕ is the reference phase of the lock in.

IV. CALIBRATION OF THE M-H LOOP SETUP

The output of the pair of secondary coils is given by

$$u = \mu_0 n V \omega (1-D)\, \frac{dM(\phi)}{d\phi}, \quad (2)$$

where n is the number of turns per unit length of the secondary coil (sample coil), V is the volume of the sample, $\omega = 2\pi f$ is the angular frequency of the applied ac field, D is the demagnetizing factor of the sample, and $M(\phi)$ is the magnetization at a phase angle ϕ. The lock-in output can be written as

$$S(\phi) = \frac{1}{2\pi} \int_0^{2\pi} u\, \theta(\phi - \phi_0)\, d\phi, \quad (3)$$

where $\theta(\phi-\phi_0)$ is a step function representing the square wave. From Eqs. (2) and (3), we get

$$S(\phi_0) = \frac{\mu_0 n V \omega (1-D)}{\pi} [M(\phi_0) - M(\phi_0+\pi)]. \quad (4)$$

For a symmetric loop with no superimposed dc field, $M(\phi_0) = -M(\phi_0+\pi)$ and hence

$$M(\phi_0) = \frac{S(\phi_0)}{4\mu_0 n V f (1-D)} = K S(\phi_0), \quad (5)$$

where $K = 1/[4\mu_0 n V f (1-D)]$ is the calibration factor. For a perfect sinusoidal field, the field values corresponding to the phase angle ϕ_0 can be computed if the amplitude of the ac field, H_m, is known using $H(\phi_0) = H_m \sin \phi_0$.

V. PHASE ADJUSTMENT

Since the shape and area of ac M-H loops depend greatly on the phase difference ϕ between M and H, all extraneous phase shifts introduced by various circuit elements should be avoided. Since it is difficult to eliminate these phase shifts as the lock in is operated in the flat-band mode and the phase is swept, a phase correction should be applied to eliminate them. For this purpose the field of initial flux entry into the sample is first determined from the field dependence of the ac susceptibility on the same sample. Then, we have recorded an M-H loop below that field, in the perfect Meissner state of the sample where $M = -H$, and adjusted the phase more precisely to get zero loop area. The same phase correction was applied for all the loops. The procedure for phase correction is discussed in more detail in Ref. 33.

VI. RESULTS AND DISCUSSION

A. General features

The ac magnetic hysteresis measurements on the sintered (A) and press sintered (B) BSCCO samples show that each of them exhibit two sets of hysteresis loops which can be identified as contributions from the intergrain and intragrain regions, respectively. Figures 1(a) and 1(b) show the isothermal field variation of ac M-H loops recorded at 77 K and 33 Hz for samples A and B, respectively.

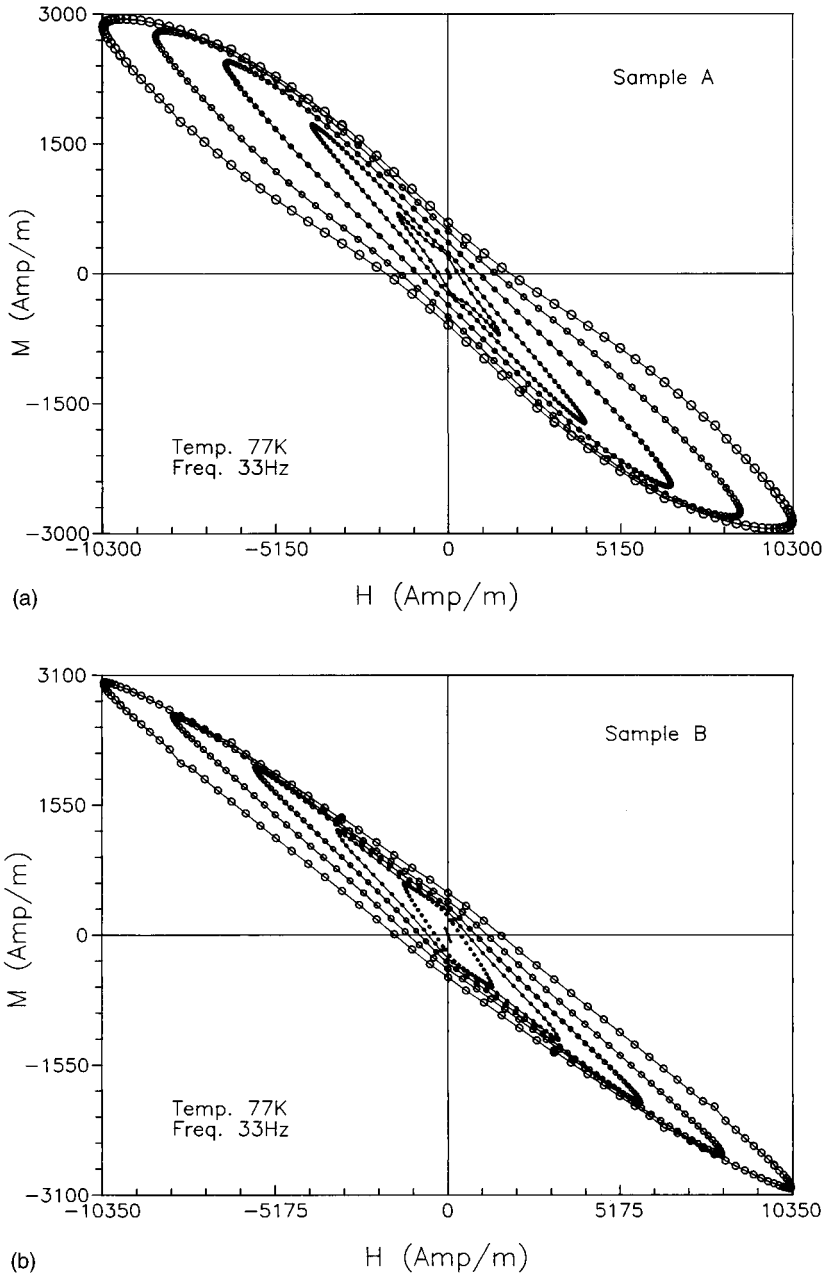

FIG. 1. Isothermal field variation of ac M-H loops recorded using the lock-in flat-band detection method at 77 K and at 33 Hz in (a) sintered and (b) press-sintered Bi 110-K-phase samples. Solid lines are a guide to the eye.

The sintered sample shows a loop opening beyond 1 Oe, from which the intergranular lower critical field H_{c1} is identified to be ~1 Oe. The intergranular loops increase in size up to the full penetration field of this region which is around H_{pi}~8 Oe, beyond which the loop collapses due to breaking up of intergranular couplings. The slope of the loop at higher fields is less than the initial slope, indicating a reduced diamagnetic behavior of the sample, and it gives the effective permeability[3] of the ceramic sample. The loop again starts opening up at higher fields due to flux entry into the grains. The intragranular loops grow in size with increase in field amplitude and develop into a bird-wing-like shape at still higher fields. Figure 2(a) shows the ac M-H loops recorded in sample A for various field amplitudes at 77 K and at 33 Hz.

In the case of press-sintered samples the intergranular loop does not collapse suddenly, but shows a gradual reduction in loop area above H_{pi}~11 Oe, the full penetration field of the intergrain region. The intergrain J_c estimated from the full penetration field shows that the coupling strength and hence the intergrain J_c have improved on press sintering. Above H_{pi} the loop assumes a rhombuslike shape with narrow wings. The intragrain loop opens up above 100 Oe, showing that there is an increase in the apparent lower critical field of the grains compared to the sintered sample.

B. Effective relative permeability μ_{cer}

The slope of the hysteresis loops beyond the vanishing of the intergrain contribution remains constant up to the lower critical field of the grains and has its origin in the diamagnetism of the grains. This slope is less than the initial diamagnetic slope of the bulk specimen ($\chi' = -1$) at low fields and is related to the effective relative permeability (μ_{cer}) of the ceramic material as given by

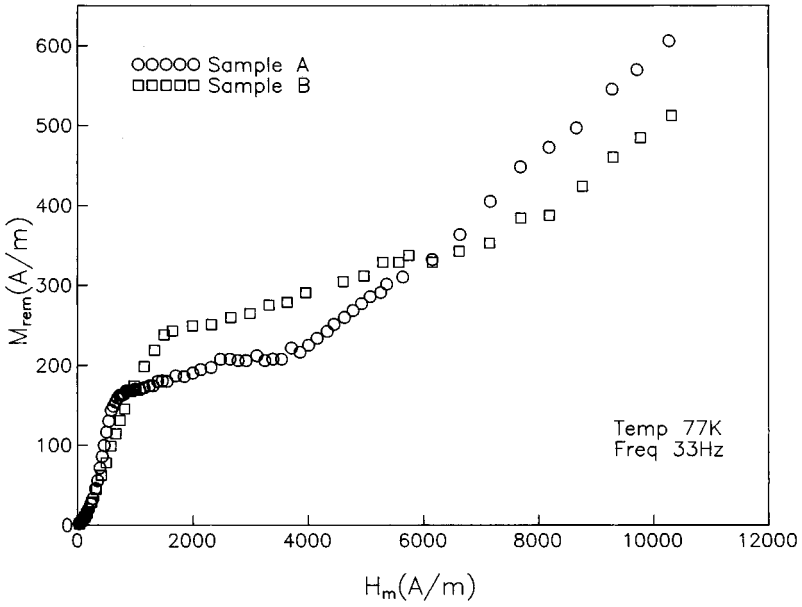

FIG. 2. Field variation of remnance at 77 K.

$$-M=\left[\frac{(1-\mu_{\rm cer})H_m}{1-(1-\mu_{\rm cer})D}\right].$$

The $\mu_{\rm cer}$ values thus derived are 0.54 and 0.64 for samples A and B, respectively. It can be seen that if the demagnetization effects are negligible, then the ratio of the reduced diamagnetic slope to the initial one directly gives the effective diamagnetic grain fraction, $f_g=1-\mu_{\rm cer}$ which was estimated to be 0.46 and 0.36 for the above samples.

C. Remnant magnetization

The value of magnetization as the ac field crosses zero gives the remnant magnetization (M_r). The remnant magnetization variation with field amplitude shows (Fig. 3) a two-step behavior for both samples, showing the granular nature of the materials. The second rise in remnance is due to flux entry into the grains and hence indicative of the lower critical field H_{c1g} of the grains. While the H_{c1g} for the sintered sample is around 50 Oe, the press-sintered sample shows an increase in H_{c1g} to about 100 Oe. The variation in H_{c1g} might have its origin in surface barrier effects.[34,35,56]

D. ac losses

The ac loss per cycle per unit volume of the sample is given by the area enclosed by the M-H loops, and is also related to the imaginary component of the fundamental ac susceptibility χ_1'' by the relation[36–38]

$$\oint MdH=\frac{(\chi_1''H_m^2)}{2\mu_0}. \tag{6}$$

The ac losses of sintered and press-sintered samples show slightly different functional dependences on field for the intergrain and intragrain contributions. For the sintered sample

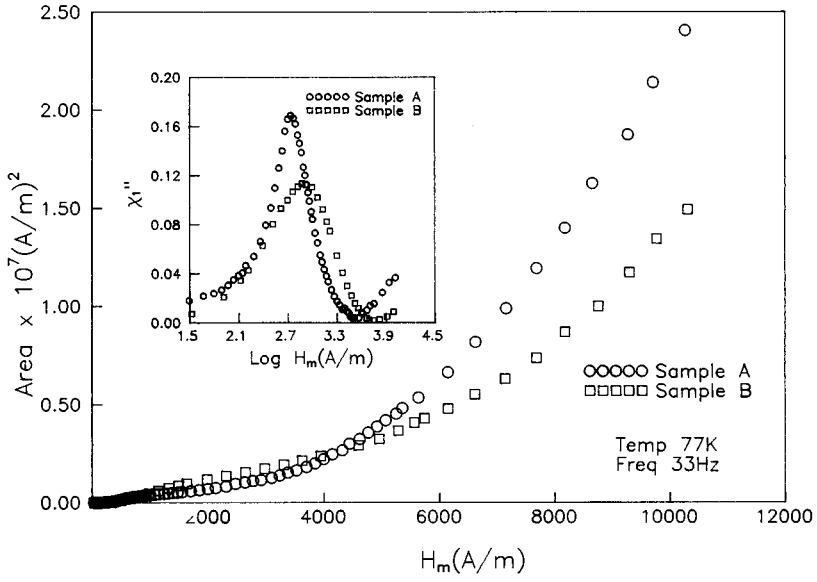

FIG. 3. Field variation ac losses and (inset) χ'' derived from ac losses at 77 K and at 33 Hz.

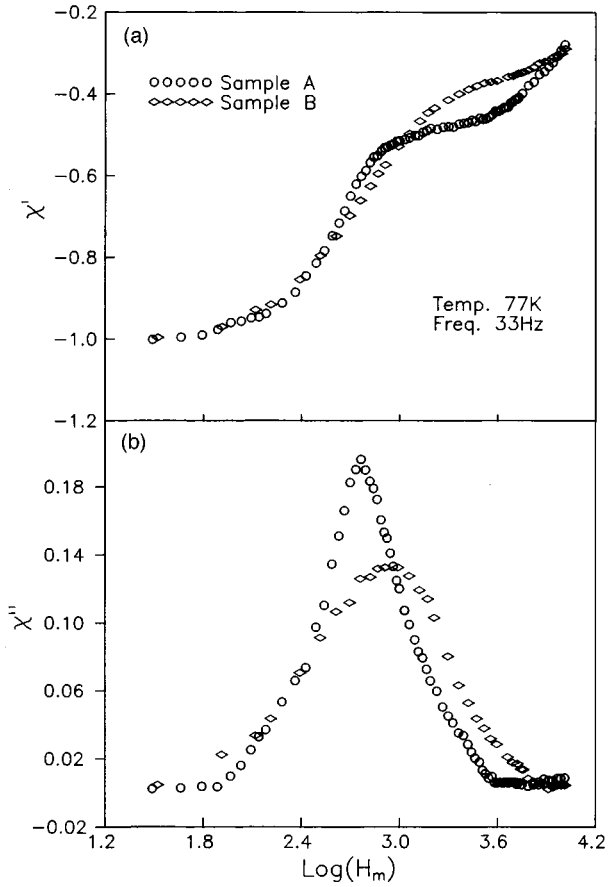

FIG. 4. Field variation of flat-band susceptibilities (a) χ' vs H_m, (b) χ'' vs H_m.

they are found to be proportional to $H^{0.48}$ and $H^{0.58}$, respectively. The intergrain loss of press-sintered sample is reduced as $H^{0.22}$ while the intragrain loss is negligible up to 150 Oe. This could be due to higher H_{c1g} and hence a reduced flux entry at that field into sample B. Figures 4(a) and 4(b) show the field variation of ac losses and χ_1'' derived from them using Eq. (5). The χ_1'' curves show that the position of the peak seen corresponds to the full penetration field and that the χ_1'' peak height has reduced on press sintering. This could be due to the reduction in porosity of the sample on press sintering which reduces the amount of trapped flux, and hence the associated loss.

E. Flat-band ac susceptibilities

For a given M-H loop recorded with $H_{ac}=H_m \sin(\omega t)$, from the zero-field value (M_r) and the peak field value (M_p) of magnetization, the flat-band ac susceptibilities χ' and χ'' are derived as M_p/H_m and M_r/H_m, respectively. The flat-band in-phase component of susceptibility χ' vs. H_m curve exhibits a two-step behavior characteristic of the ceramic (weak-link) nature of the sample. The flat-band out-of-phase component of susceptibility (χ'') plotted as a function of H_m [Fig. 5(b)] shows peak at 8 Oe and 11 Oe, respectively, for samples A and B, which are the full penetration fields of the intergranular region. Reduction in peak height on press sintering is also evident from Fig. 5(b) as seen in Fig. 4(b).

F. Harmonics

The various shapes exhibited by the M-H loops of sintered and press-sintered samples are due to the generation of higher harmonics in these materials. By doing a fast Fourier transform (FFT) on the M vs time curve, the real and imaginary components of the various harmonics of magnetization and hence the susceptibility are obtained. While the χ_n' vs H_m curve thus obtained shows [Figs. 5(a) and 5(b)] a two-step behavior, the higher-harmonic components of χ_n' exhibit a minima (negative maximum) whose position shifts towards higher fields with increase in the order of harmonics. The third-harmonic component of χ_n'' [Figs. 5(c) and 5(d)] is 3 times larger than the higher-order harmonics and hence plays a major role in determining the shape of the hysteresis loops. While the third-harmonic susceptibility of the sintered sample shows an asymmetric peak, the press-sintered sample shows a nearly symmetric peak. The fifth-harmonic susceptibility χ_5'' exhibits a derivativelike shape. Here also the asymmetry in the curve has reduced on press sintering. This could be indicative of the nature of the variation of J_c with field. Ishida and Goldfarb have studied in detail the field and temperature variations of harmonic susceptibilities by recording them individually. Comparison of the field variation of odd-harmonic susceptibilities with similar studies reported in the literature[39–42] show that our results differ from the weakly coupled loop model of Ishida and Mazaki.[42]

G. Flux profile

From the peak field value of magnetization (M_p), the flux profiles[20,43] inside the ceramic sample (beyond the London penetration depth) are constructed by plotting the deviation of the slope of M_p vs H_m curve from -1 as a function of H_m (Fig. 6). In the case of the sintered sample, the normalized penetration depth (p/R) increases with field, showing a maximum at the full penetration field of 8 Oe. Here R is the radius of the cylindrical sample. The penetration remains constant between 10 Oe and 50 Oe as the flux entry is already complete into the bulk of the material and is confined to within the London penetration depth of the diamagnetic grains. The penetration changes above 50 Oe due to flux entry into the grains. The maximum penetration occurs at around 11 Oe for press-sintered sample and the penetration remains constant from 20 Oe to around 100 Oe, above which it changes again due to the flux entry into the grains. μ_{cer} can be estimated[44] from the intercept (p^*) obtained on extrapolation of the region of constant p of the flux profiles to the zero-field axis as $\mu_{cer}=(1-p^*/R)$. The values of μ_{cer} thus obtained compare very well with those determined from the reduced diamagnetic slope of the hysteresis loops.

H. Theoretical modeling of M-H loops

The magnetic behavior of conventional type-II superconductors is explained by Bean's model[45] which assumes the J_c to be field independent. But the critical current density of high-T_c superconductors is strongly field dependent and hence, in general, Bean's model fails. Several critical state models have been proposed in the literature[46–53,3] by assum-

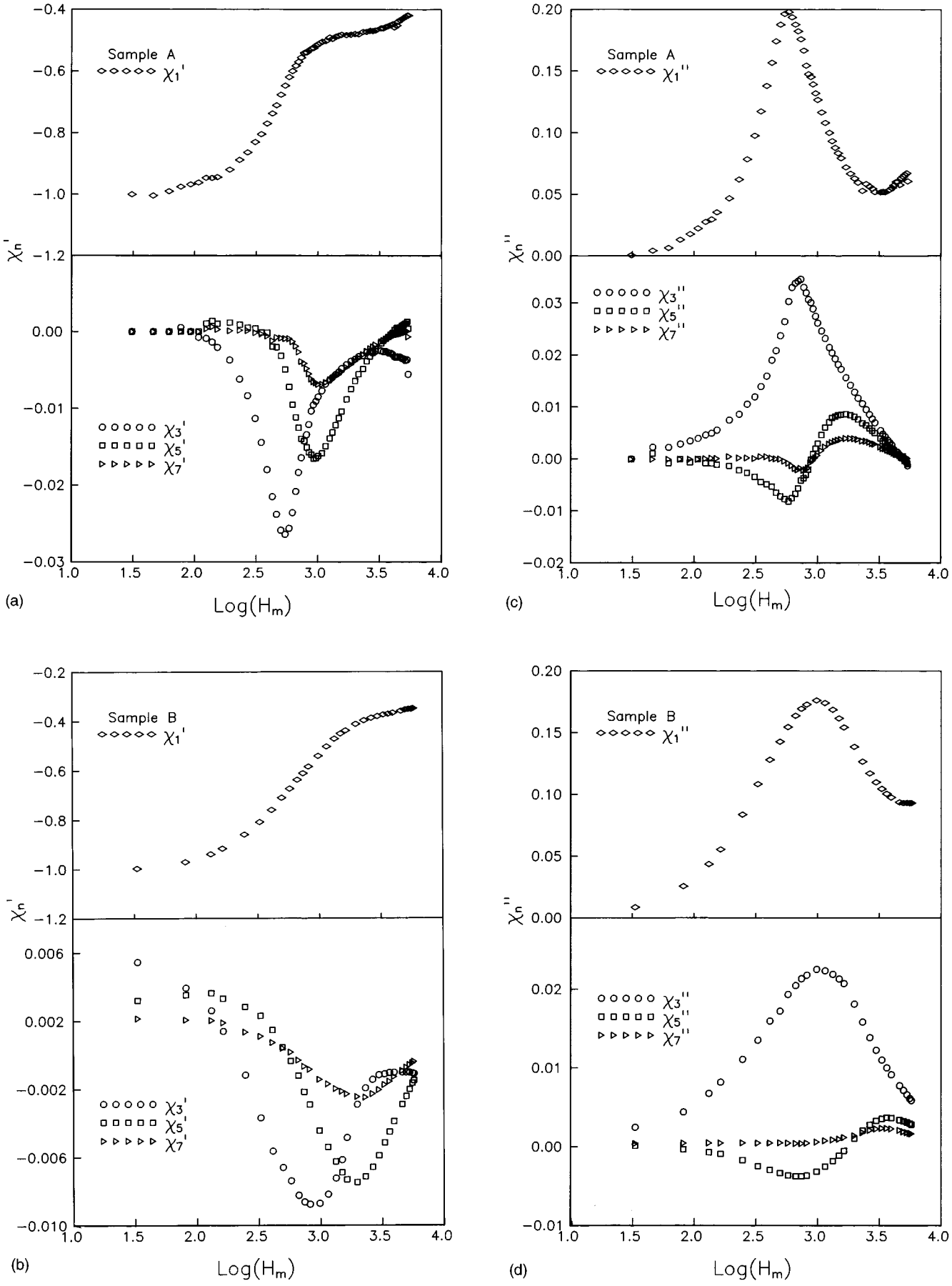

FIG. 5. Field variation of odd harmonic susceptibilities (a), (b) χ_n' vs H_m and (c), (d) χ_n'' vs H_m derived from the M vs time curve by doing a fast Fourier transform.

ing different functional dependences for J_c on H to explain the observed magnetic behavior. We have analyzed our data using Kim's model[46,54]

$$\left[J_c(H_i)=\frac{K}{|H_i|+H_0}\right]$$

and the exponential model[51–53,55]

$$\left[J_c(H_i)=J_0\ \exp\left(-\frac{|H_i|}{H_0}\right)\right],$$

where K, H_0, and J_0 are constants and H_i is the local internal field. In this approach the local magnetization M_i is considered as the field produced by the bulk supercurrents flowing in the material and is given by $M_i=H_i-H$, where H is the applied field. The total field magnetization M is the average of M_i over the cross section.[54,55] The local field H_i is derived in terms of the applied field and supercurrent densities.

Since the magnetization of granular superconductors has contributions from the superconducting grains and also their interconnections, the measured magnetization $M(H)$ can be written as[1,7,8]

$$M(H)=f_g M_g(H)+(1-f_g)M_m(H), \tag{7}$$

where $M_g(H)$ is the magnetization of the diamagnetic grains and M_m is the contribution to the magnetization from the matrix due to intergranular Josephson currents. For low applied fields $M_g=-H$ because the susceptibility of grains, χ_g, is almost equal to -1. For higher applied fields, weak links become normal and $M_m(H)$ tends to zero.

For simulating the M-H loops to critical state models, the f_g value needs to be determined. Unlike in the case of ac susceptibility analysis[10,11] where f_g was normally taken as a free parameter of the fit, in the present work f_g is determined from the slope of the hysteresis loop at loop closure. By assuming $M_g(H)=-H$ in Eq. (7), the measured M-H loops for $H_m\simeq$500, 1000, and 1500 A/m, which are mainly due to intergranular matrix, could be fitted very well to Kim's model for sample A and the exponential model for sample B as shown in Figs. 7(a) and 7(b). The parameters obtained form the field variation of intergrain M-H loops and J_c values at 77 K are given in the Table I.

The above fits were carried out without any modification of the as-measured data. This is in contrast to Dersh and Blatter's[3] approach in which they have extrapolated and subtracted the narrow wings of the loop and then the modified loop was fitted assuming $J_c(H_i)=J_0[1-(|H_i|/H_p)]\,\theta(H_p-|H_i|)$ where H_i is the local magnetic induction and $\theta(x)$ denotes the Heaviside step function. They regarded the wings to be due to the contribution from voids in the material which cannot be accounted for in their model.

While the intergranular loops of sample A could be directly fitted to Kim's model, to simulate the intragranular loops of this sample the surface-barrier-modified equilibrium magnetization M_s has to be taken into account. According to Chen *et al.*[56] the descending branch of $M_s(H)$ can be defined as

$$M_s(H)=-H+H_m-H_3-(H_1-H_3)\exp\frac{(H_1-H_m)}{H_4}$$

$$\text{for } (H_{m'}<H<H_m), \tag{8a}$$

$$M_s(H)=-H_3-(H_2-H_3)\exp\frac{(H_2-H)}{H_4}$$

$$\text{for } (H_2<H<H_{m'}), \tag{8b}$$

$$M_s(H)=-H \quad \text{for } (-H_1<H<H_2), \tag{8c}$$

$$M_s(H)=H_3+(H_1-H_3)\exp\frac{(H_1+H)}{H_4}$$

$$\text{for } (-H_m<H<-H_1), \tag{8d}$$

where $H_{m'}$ is the field at which the first change of slope occurs in the descending branch of $M_s(H)$, H_1 and H_2 are the fields for the first flux entry and last flux exit, respectively, $-H_3$ is the value of equilibrium magnetization at H_m,

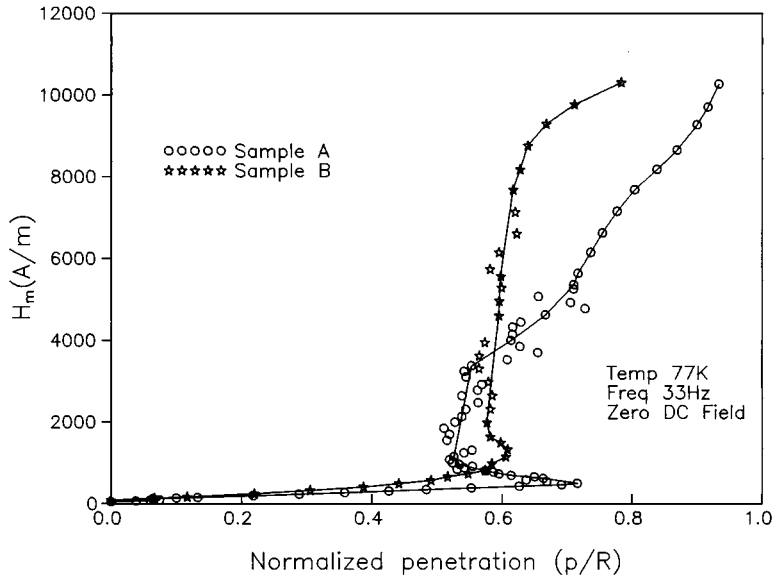

FIG. 6. Flux profiles in the sintered and press-sintered samples derived from the slope of the M_{peak} vs H_m curve. Solid lines are a guide to the eye.

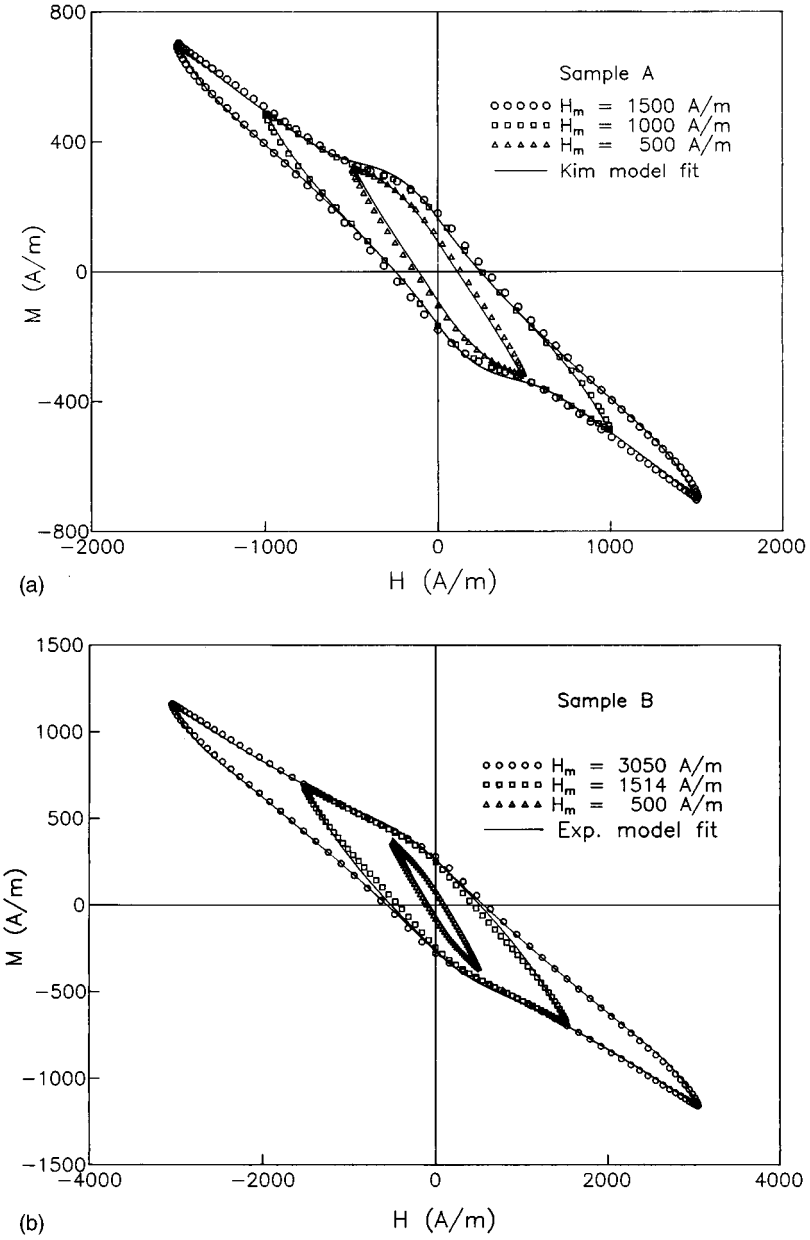

FIG. 7. Theoretical simulation of the intergranular loops of (a) sintered and (b) press-sintered samples using the Kim and exponential models.

and H_4 accounts for the field variation of $M_s(H)$. The measured M-H loops for $H_m \geqslant 1500$ A/m which are mainly due to superconducting grains were fitted by assuming $M_m(H)=0$ in Eq. (7) and by considering $M_g(H)$ to be the sum of bulk magnetization predicted by the critical state models (Kim, exponential models) and $M_s(H)$ (Fig. 8). H_p, p, H_1, H_2, and H_3 were taken as free parameters of the fit while value for H_4 was assumed such that the slope of the experimental curve matches with that of theoretical M-H loop. The fit parameters are $H_p=12\,863$ A/m, $p=5.3$, $H_1=4340$ A/m, $H_2=411$ A/m, $H_3=557$ A/m, and $H_4=10\,345$ A/m. The analysis of intragranular loop shows the presence of surface barrier effects and such an observation has been made in the literature for YBCO (Ref. 56) and the 85 K phase of BSCCO (Ref. 57), also.

Unlike for sample A with an apparent H_{c1g} (the lower critical field of grains) of 50 Oe, the apparent granular H_{c1g} is around 100 Oe for sample B. The M-H loop for sample B at 150 Oe can be seen to be elliptical in shape with a smaller opening which could be due to lack of considerable flux entry into the grains. We find that this loop can be simulated very well by Kim's model as well as the exponential model without incorporating the surface barrier modification (Fig. 9). The fit parameters are given in Table I.

The intergranular pinning force density, F_p, was estimated using the relation $F_p=J_c(H_i)B_i$, where the field variation of critical current density $J_c(H_i)$ was calculated using the Kim and exponential models for samples A and B, respectively, and using the parameters obtained from the fit of intergranular M-H loops. The maximum values of F_p obtained for samples A and B are, respectively, 7.0×10^2 and 2.5×10^3 TA/m^2, which suggests an improved pinning strength upon press sintering. The reason for this could be that the centers responsible for pinning the flux in the intergranular region, which need to be of the order coherence length, are enhanced in density on press sintering. Unlike in the sintered sample with 50% porosity and larger-sized grains, it is quite possible that pinning centers that can effec-

TABLE I. List of parameters obtained from the theoretical fits.

Sample	Intergrain/intragrain	Model	f_g	H_p (A/m)	p	J_c (77 K) (A/cm^2)
Sintered	inter	Kim's model	0.44	650	4.5	65
Press sintered	inter	exponential model	0.36	1070	0.8	100
Sintered	intra	exponential model[a]	0.37	12 863	5.28	2.57×10^5
Press sintered	intra	exponential model	0.36	21 021	18.705	2.1×10^6

[a]With surface barrier modification.

tively cause pinning are more in press-sintered samples with much reduced porosity (15%) and smaller grains.

VII. CONCLUSIONS

The f_g values determined from M-H loop measurements show that there is little change in its value on press sintering even though there is a large reduction in porosity. This could be due to smaller grains in the press-sintered sample. The flow of supercurrents on the surfaces of each of the smaller grains can cause a reduction in the effective volume fraction of the grains which compensated for the increase in the solid fraction of the sample (50%–85%) on press sintering. The critical current density (J_{ci} and J_{cg}) values estimated from M-H loops show that both the J_{ci} and J_{cg} get enhanced on press sintering. The rise in J_{ci} could be due to the increase in coupling strength of the linkages between the grains. The lower J_{cg} of sample A compared to that of sample B may be due to the lower H_{c1g} (50 Oe), which allows the flux entry into the grains at 150 Oe, and that the J_{cg} is probably field dependent. The field dependence of J_{cg} is also suggested by the nonlinearity of the flux profile above its H_{c1g}. The intergranular loops of sintered and press-sintered samples show

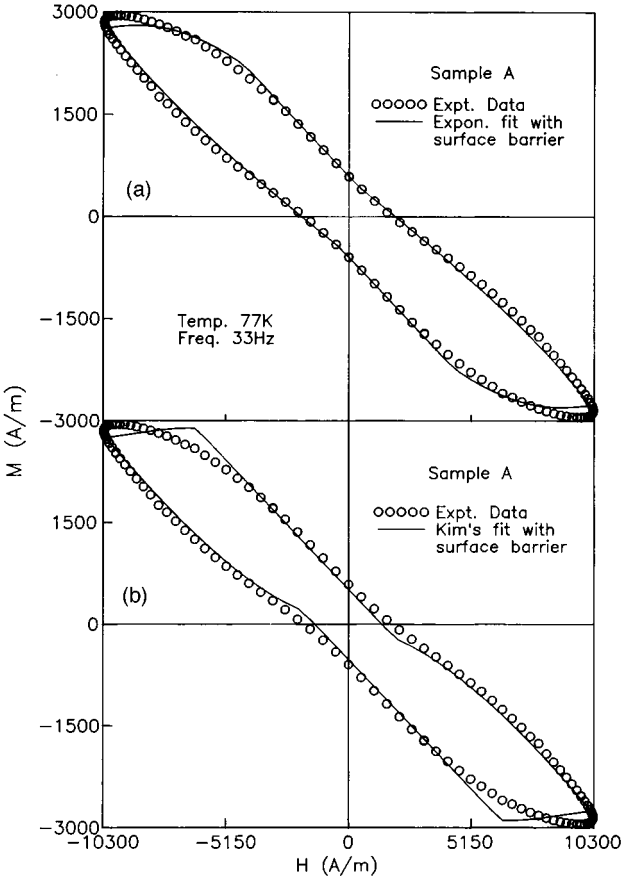

FIG. 8. (a) Exponential and (b) Kim model fits with surface barrier modification to an intragranular loop of sintered Bi 110 K phase.

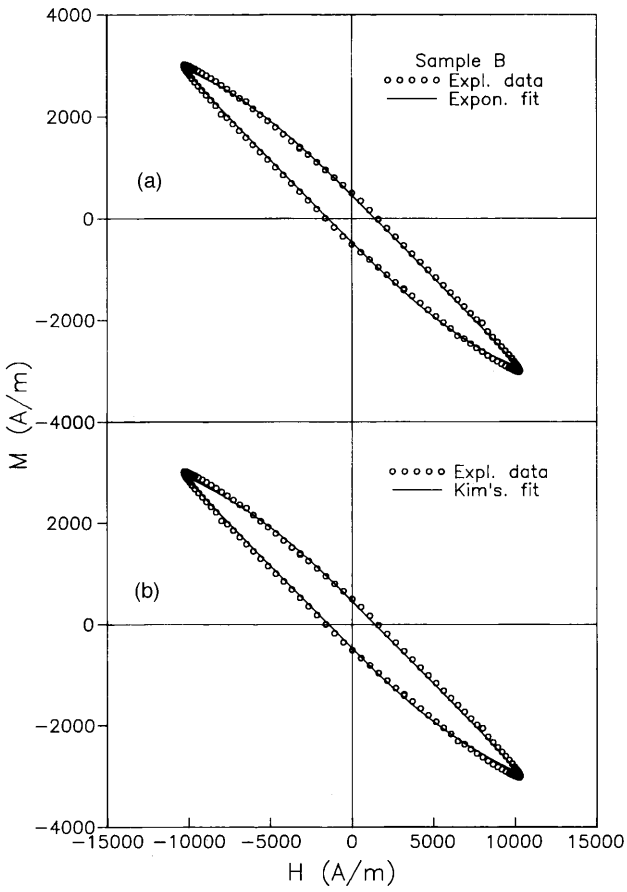

FIG. 9. (a) Exponential and (b) Kim model fits to an intragranular loop of a press-sintered Bi 110 K phase sample.

an excellent fit to the Kim and exponential models, respectively, and there was no need for subtraction of the wings as proposed by Dersch and Blatter. The enhancement in the apparent lower critical field H_{c1g} value on press sintering can be attributed to an enhanced surface barrier effect due to an improved microstructure of the sample which could have resulted in a reduction in the defects around the grain boundaries.[35] To simulate the intragranular loops the surface-barrier-modified equilibrium magnetization has been incorporated in addition to the bulk magnetization predicted by the Kim and exponential models and we find that the exponential model gives a better fit than the Kim model. The fit could possibly be improved if a distribution in the full penetration fields, either due to the presence of grain clusters or due to a variation in grain sizes about an average value, is taken into account. However, the qualitative features are very well reproduced. A harmonics study shows that the sharpness in the field variation of harmonic susceptibilities and their magnitude were reduced on press sintering, indicating that the harmonics generation is a manifestation of the weak-link nature of the material. Based on our analysis of the magnetic response we find that magnetic properties like the intergranular critical current density (J_{ci}), the apparent lower critical field of the grains (H_{c1g}), intragranular critical current density (J_{cg}), and hysteresis in magnetization are strongly dependent on the microstructure which can be altered by adopting different preparation techniques.

ACKNOWLEDGMENTS

This work is supported by the Department of Science and Technology, Government of India. One of the authors (N.H.K.) wishes to acknowledge the Council of Scientific and Industrial Research, New Delhi for financial support. We thankfully acknowledge N. Hari Babu and Dr. S. Ravi for helpful discussions.

[1] J. R. Clem, Physica C **153–155**, 50 (1988).
[2] John R. Clem, B. Bumble, S. I. Raider, W. G. Gallagher, and Y. C. Shih, Phys. Rev. B **35**, 6637 (1987).
[3] H. Dersch and G. Blatter, Phys. Rev. B **38**, 11 391 (1988).
[4] M. Murakami, M. Morita, K. Doi, and M. Myamoto, Jpn. J. Appl. Phys. **28**, 1189 (1989).
[5] T. Asano, K. Y. Tanaka, M. Fukutomi, K. Jikihara, J. Machida, and H. Maeda, Jpn. J. Appl. Phys. **27**, 1652 (1988).
[6] M. Nikolo and R. B. Goldfarb, Phys. Rev. B **39**, 6615 (1989).
[7] K. H. Müller, Physica C **159**, 717 (1989).
[8] D. X. Chen, Yu Mei, and H. Luo, Physica C **167**, 317 (1990).
[9] O. F. Schilling, K. Aihara, A. Soeta, T. Kauro, and S. Matsuda, Phys. Rev. B **47**, 8096 (1993).
[10] S. Ravi and V. Seshu Bai, Phys. Rev. B **49**, 13 082 (1994).
[11] S. Ravi and V. Seshu Bai, Physica C **230**, 51 (1994).
[12] A. K. Grover, C. Radhakrishnamurthy, P. Chaddah, G. Ravikumar, and G. V. Subba Rao, Pramana J. Phys. **30**, 569 (1988).
[13] I. E. Edmond and L. D. Firth, J. Phys. Condens. Matter **4**, 3813 (1992).
[14] R. Maury, A. R. Fert, J. P. Redoules, J. Ayache, J. Sabras, and C. Monty, Physica C **167**, 591 (1990).
[15] R. Navarro, F. Lera, C. Rillo, and J. Bartolome, Physica C **167**, 549 (1990).
[16] P. Fabricatore, U. Gambardella, F. Gömöry, R. Musenich, M. Occhetto, R. Parodi, and P. Pompa, Rev. Sci. Instrum. **62**, 1796 (1991).
[17] S. K. Ghatak, A. Mitra, and D. Sen, Phys. Rev. B **45**, 951 (1992).
[18] Fedor Gömöry, Rev. Sci. Instrum. **62**, 2019 (1991).
[19] G. E. Gough, M. S. Colclough, D. A. O'Conner, F. Wellhofer, N. McN. Alford, and T. W. Button, Cryogenics **31**, 119 (1991).
[20] A. M. Campbell, J. Phys. C **2**, 1492 (1969).
[21] R. B. Goldfarb, A. F. Clark, A. Z. Braginski, and A. J. Panson, Cryogenics **27**, 475 (1987).
[22] H. Küper, I. Apfelstedt, W. Schuer, R. Flükiger, R. Meier Hirmer, and H. Wühlz, Z. Phys. B **69**, 159 (1987).
[23] F. Gömöry and P. Lobotka, Solid State Commun. **66**, 645 (1988).
[24] S. D. Murphy, K. Renouard, R. Crittenden, and S. M. Bhagat, Solid State Commun. **69**, 367 (1989).
[25] Q. H. Lam, Y. Kim, and C. D. Jeffries, Phys. Rev. B **42**, 4846 (1990).
[26] D. X. Chen, A. Sanchez, T. Puig, L. M. Martinez, and J. S. Mũnoz, Physica C **168**, 652 (1990).
[27] J. M. Tarascan, Y. Le Page, P. Barboux, B. G. Bagley, L. H. Greene, W. R. McKinnon, G. W. Hull, M. Giroud, and D. M. Hwang, Phys. Rev. B **37**, 9382 (1988).
[28] X. Z. Wang, K. Donnelly, T. Bakas, J. M. D. Coers, I. Roseman, and C. Simon, Solid State Commun. **69**, 829 (1989).
[29] J. M. Tarascan, P. Barboux, L. H. Greene, B. G. Bagley, G. W. Hull, Y. Ze Page, and W. R. McKinnon, Physica C **153**, 566 (1988).
[30] F. Shi, T. S. Rong, S. Z. Shou, X. F. Wu, J. Du, Z. H. Shi, C. G. Cui, R. Y. Jin, J. L. Zhang, Q. Z. Ran, and N. C. Shi, Phys. Rev. B **41**, 6451 (1990).
[31] V. Seshu Bai, S. Ravi, T. Rajasekharan, and R. Gopalan, J. Appl. Phys. **70**, 4378 (1991).
[32] C. W. Crabtree, Phys. Rev. B **16**, 1117 (1977).
[33] N. Harish Kumar, Ph.D. thesis, University of Hyderabad, 1996.
[34] C. P. Bean and J. D. Livingston, Phys. Rev. Lett. **12**, 14 (1964).
[35] R. W. De Blois and W. De Sorbo, Phys. Rev. Lett. **12**, 499 (1964).
[36] K. V. Bhagwat and P. Chaddah, Physica C **166**, 1 (1990).
[37] M. N. Wilson, *Superconducting Magnets* (Clarendon Press, Oxford, 1983), p. 162.
[38] Hongbo Jiang and Charles P. Bean, Rev. Sci. Instrum. **66**, 3284 (1995).
[39] T. Ishida and R. B. Goldfarb, Phys. Rev. B **41**, 8937 (1990).
[40] T. Ishida, R. B. Goldfarb, S. Okayasu, Y. Kazumata, J. Franz, T. Arndt, and W. Schaner, Mater. Sci. Forum **137–139**, 103 (1993).
[41] L. Ji, R. H. Sohn, G. C. Splading, C. J. Lobb, and M. Tinkham, Phys. Rev. B **40**, 10 936 (1989).
[42] T. Ishida and H. Mazaki, J. Appl. Phys. **52**, 6798 (1981).
[43] A. M. Campbell and F. J. Blunt, Physica C **172**, 253 (1990).
[44] A. M. Campbell, in *Magnetic Susceptibility of Superconductors and Other Spin Systems*, edited by R. A. Hein *et al.* (Plenum Press, New York, 1970), p. 147.

[45] C. P. Bean, Phys. Rev. Lett. **8**, 250 (1962).
[46] Y. B. Kim, C. F. Hempstead, and A. R. Strand, Phys. Rev. Lett. **9**, 306 (1962).
[47] S. F. Wahid and N. K. Jaggi, Physica C **184**, 88 (1991).
[48] J. H. P. Watson, J. Appl. Phys. **39**, 3406 (1968).
[49] F. Irie and K. Yamafuji, J. Phys. Soc. Jpn. **23**, 255 (1967).
[50] I. M. Green and P. Hlawiczka, Proc. IEEE **114**, 1329 (1967).
[51] W. A. Fietz, M. R. Beasley, J. Silcox, and W. W. Webb, Phys. Rev. **136**, A335 (1964).
[52] V. R. Karasik, N. G. Vasilev, and V. G. Ershov, Sov. Phys. JETP **32**, 433 (1971).
[53] G. Ravi Kumar and P. Chaddah, Phys. Rev. B **39**, 4704 (1989).
[54] D. X. Chen and R. B. Goldfarb, J. Appl. Phys. **66**, 2489 (1989).
[55] D. X. Chen, A. Sanchez, and J. S. Muñoz, J. Appl. Phys. **67**, 3430 (1990).
[56] D. X. Chen, R. W. Cross, and A. Sanchez, Crogenics **33**, 695 (1993).
[57] S. Uma, S. Ravi, and G. Rangarajan, Physica C **250**, 225 (1995).